

Sixth World Conference on Structural Control and Monitoring

Proceedings of the 6th edition of the World Conference of the International Association for Structural Control and Monitoring (IACSM), held in Barcelona, Spain

15-17 July 2014

Edited by:

J. Rodellar

Universitat Politècnica de Catalunya-BarcelonaTech, Spain

A. Güemes

Universidad Politécnica de Madrid, Spain

F. Pozo

Universitat Politècnica de Catalunya-BarcelonaTech, Spain

A publication of:

**International Center for Numerical
Methods in Engineering (CIMNE)**

Barcelona, Spain



Experimental and Numerical Studies of Magnetorheological Fluids

Jerzy Rojek¹, Grzegorz Mikułowski² and Izabela Marczevska³

Abstract

This paper presents experimental and numerical studies of magnetorheological (MR) fluids. Experimental studies have been focused on the investigation of MR fluid flow in the valve mode. An experimental device operating in the valve mode has been built and used for testing. Numerical investigations have included analysis of magnetic field, continuum based analytical modelling of the valve mode as well as micromechanical discrete element simulation of MR fluid. Analytical studies of the MR flow have been carried out using the conventional Buckingham equation with constant yield stress across the valve gap and the modified Buckingham equation with nonlinear yield stress distribution across the channel according to the magnetic field distribution determined numerically. The analytical results have been compared with experimental data. A better performance of the modified Buckingham model has been observed. A micromechanical model of MR fluids has been developed within the discrete element framework. The DEM model has been verified qualitatively on a test example of forming chains by magnetized particles after application of an external magnetic field.

I. INTRODUCTION

Magnetorheological (MR) fluids, suspensions of microscopic magnetic particles in carrier liquids, belong to the class of intelligent or “smart” materials which can respond to some external stimuli. Their mechanical properties can be reversibly changed and controlled by external magnetic field, which is exploited in active and semiactive control systems. MR fluids have a wide range of applications such as automotive clutches, brakes, actuator systems, vibration dampers, control valves, and shock absorbers. Modeling and numerical simulation of MR fluids and devices are still challenges in the current research [1].

This paper presents experimental and numerical studies of MR fluids. Experimental studies presented in this paper have been focused on the valve mode. The valve or flow mode is one of the operational modes of magnetorheological fluids, in which the fluid is under pressure gradient in a duct at the same time being excited with an externally applied magnetic field in the transverse direction. The flow mode is typical for a variety of applications of MR fluids. It is widely utilized in the class of applications devoted to semi-active damping e.g. military vehicle suspension shock-absorbers [2], sport cars suspension [3] or adaptive landing gears [4], [5], [6]. In this context, experimental verification of the MRF behaviour under the flow mode of operation is of great practical importance.

II. EXPERIMENTAL STUDIES OF MAGNETORHEOLOGICAL FLUIDS

A. Overview of the experimental set-up

The investigation of the MRF in the flow mode was conducted on an own experimental model of a magnetic valve (Figure 1). The magnetic valve was designed so as to enable the following measurements: determination of pressure drop variation as a function of the magnetic field intensity and volumetric flow rate of the fluid. The valve also enables visualization of the MR fluid in flow mode.

The experimental volume of the MR flow channel that was activated by the magnetic field is in the form of a rectangular block as it is shown in Figure 2. The fluid in the channel was excited by the magnetic field with lines along the Y axis and the fluid was under a pressure gradient along the X axis (Figure 2). The dimensions of the channel were: 1 mm height, 3 mm width and the magnetically active length was 20 mm. Figure 1(b) presents the top view of the experimental valve. The top surface of the device is made of glass in order to enable the MR fluid flow observations. The dark grey area visible in Figure 1(b) represents the MR fluid. The channel's side borders are formed by six plates. Four of them are aluminium plates (having non-magnetic properties) and two of them are made of silicon iron and play the role of magnetic poles, connected to the magnetic circuit (Figure 3).

The magnetic circuit was designed in a way to provide a sufficient magnetic field to excite the MR fluid across the orifice. The magnetic circuit consisted of a magnetic core made of silicon iron and a coil (Figure 3). The main part of the core had cross section 20 mm x 10 mm (width x height) and for the part that was connected to the experimental channel, the dimensions were reduced to 20 mm x 1 mm (width x height). The coil had 140 turns and was positioned symmetrically in reference to the gap in the magnetic circuit. The magnetic excitation system was able to generate $B = 0.6$ T between the poles. The symmetrical positioning of the coil allowed the generation of an exactly equal level of flux density on both

*This work was supported by National Science Centre of Poland, project no. 2012/05/B/ST8/02971

¹Jerzy Rojek is with the Institute of Fundamental Technological Research of Polish Academy of Sciences, Pawinskiego 5B, 02-106 Warsaw, Poland
Jerzy.Rojek@ippt.pan.pl

²Grzegorz Mikułowski is with the Institute of Fundamental Technological Research of Polish Academy of Sciences, Pawinskiego 5B, 02-106 Warsaw, Poland
gmikulow@ippt.pan.pl

³Izabela Marczevska is with the Institute of Fundamental Technological Research of Polish Academy of Sciences, Pawinskiego 5B, 02-106 Warsaw, Poland
imar@ippt.pan.pl

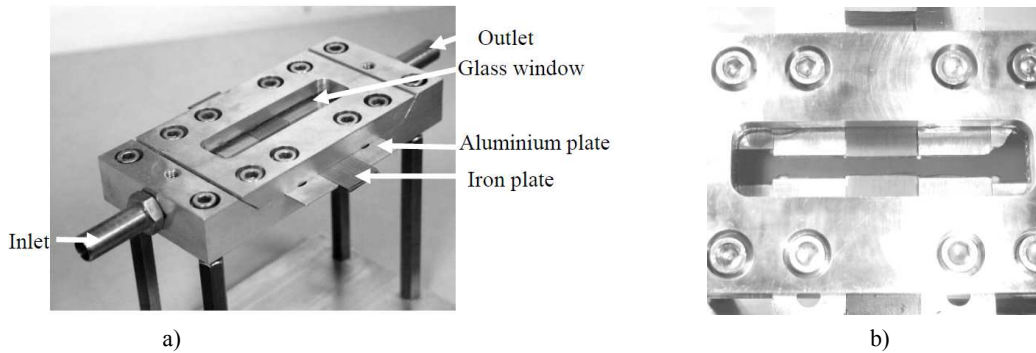


Fig. 1. Magnetorheological valve: a) general view, b) detail

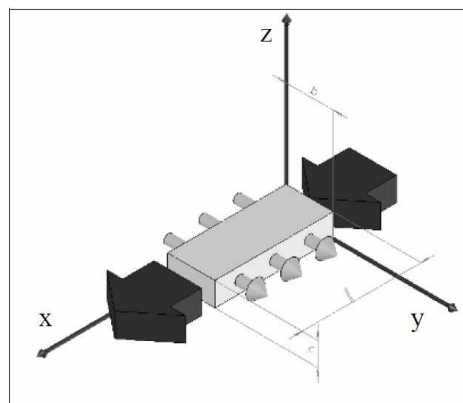


Fig. 2. Schematic representation of the active volume of the MR fluid (round arrows – magnetic induction, rectangular arrows – pressure gradient)

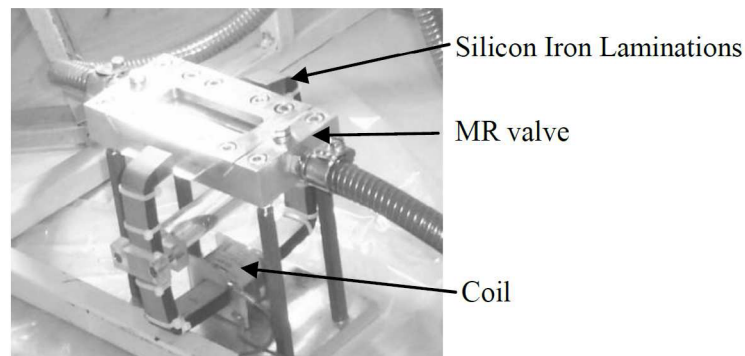


Fig. 3. Laboratory stand

surfaces of the poles. The pressure gradient was generated by a piston pump, which could produce a maximum level of 2MPa. The resulting volumetric flow rates that were tested were up to $2.5 \cdot 10^{-5} \text{ m}^3/\text{s}$.

The experiments included the following measurements: pressure signal on the inlet and outlet of the flow channel, displacement of the pump piston, and the current applied to the coil. This allowed us to obtain the quasi-steady pressure/flow rate characteristics of the investigated valve.

B. Experimental results

Magnetorheological fluid flow pattern in the magnetic valve is shown in Figure 4. The pressure/flow rate characteristics are presented in Figure 5. The pressure drop is plotted versus volumetric flow rate for a range of current excitations, which resulted in generation of steady flux densities. The obtained results will serve as the reference data for verification of the adopted mathematical and numerical models.

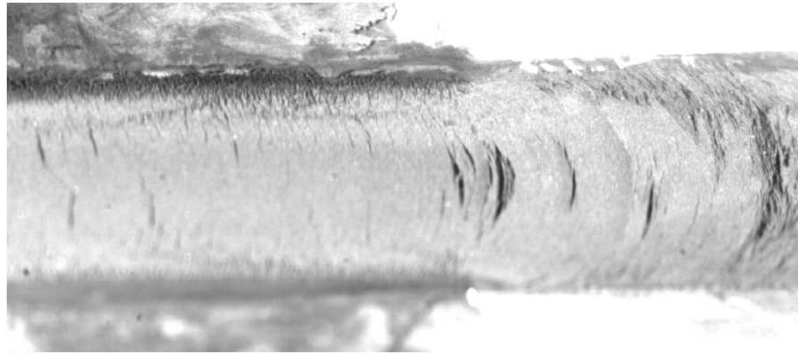


Fig. 4. Magnetorheological fluid flow in the channel

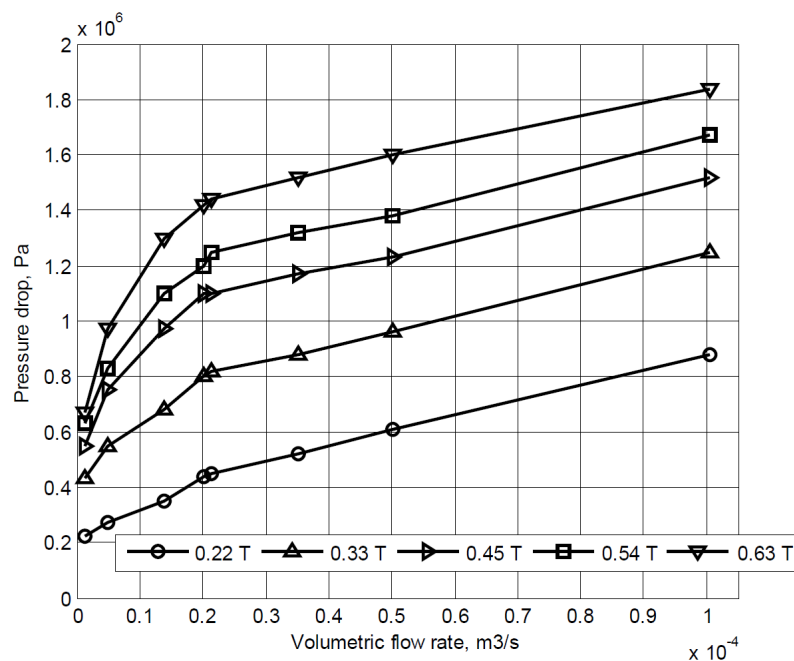


Fig. 5. Pressure drop versus displacement characteristics of the MR valve

III. MAGNETIC FIELD ANALYSIS

The MR fluid properties and flow depend on the magnetic field. In many papers devoted to the analysis of MR fluid flow in the valve mode, an invariable distribution of the magnetic flux across the valve gap is assumed, cf. [7]. The assumption is valid for a significant number of the MR devices in which the dimension of the gap is small and the field intensity is high. However, in the case when the flux density variation is significant and cannot be assumed as constant, conventional models will not predict the behavior accurately [8]. Such cases are more likely to occur in devices where the gap size is large. Then, an analysis of the magnetic field should be performed in order to obtain a more accurate distribution of the magnetic field in the valve gap.

A finite element model of the magnetic circuit described in Section II is shown in Fig. 6. The planar model accounts for the fill factor of the steel laminations, and the flux leakage into the surrounding air. The analysis was performed using the finite element software FEMM [9]. Predicted flux density distributions across the valve gap for different current values are plotted in Fig. 7. The numerical model has been validated using experimental flux density measurements in the centre of the valve gap.

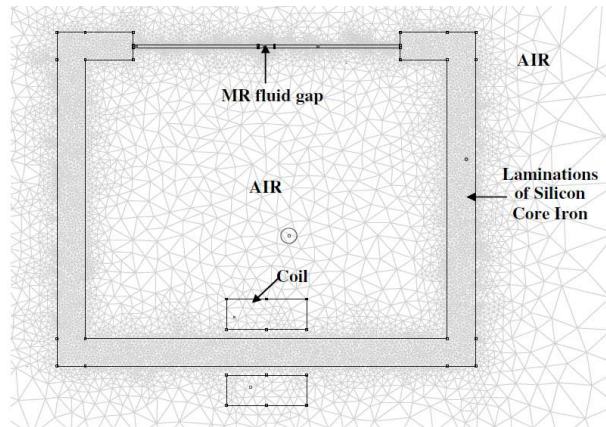


Fig. 6. Finite element model of the magnetic circuit

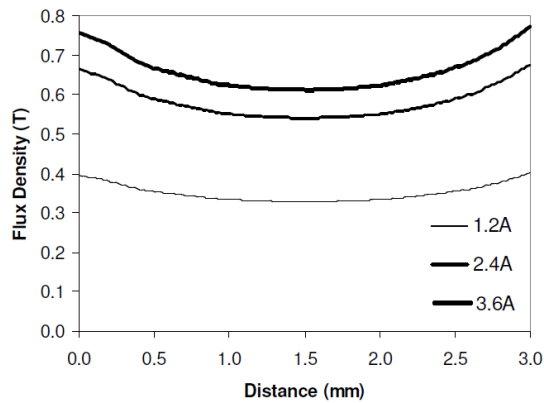


Fig. 7. Predicted flux density distribution across the valve gap

IV. ANALYTICAL MODELLING OF MAGNETORHEOLOGICAL FLUID FLOW

Magnetorheological fluid flow can be described using the Navier-Stokes equations for a non-Newtonian fluid [10]. Let us treat a MR flow in a valve mode as a 2D flow of an incompressible non-Newtonian fluid between two parallel plates separated by a distance h equal to the valve gap (Fig. 8). Assuming the flow is uni-directional ($v = 0$, v being the velocity perpendicular to the plates), steady ($\partial u/\partial t = 0$, u being the velocity parallel to the plates) and uniform ($\partial u/\partial x = 0$) under a pressure gradient imposed in the direction x parallel to the plates, we can simplify the Navier-Stokes equations to the following form:

$$\frac{\partial p}{\partial x} = \frac{\partial \tau_{yx}}{\partial y} \quad (1)$$

$$\frac{\partial p}{\partial y} = 0 \quad (2)$$

where τ_{yx} is the shear stress in the fluid. Assuming a constant pressure drop along the length l , Eq. (1) can be written in the following form

$$\frac{\Delta p}{l} = \frac{d\tau_{yx}}{dy} \quad (3)$$

To solve Eq. (3) the constitutive law for the Bingham viscoplastic material is introduced:

$$\tau_{yx} = \tau_0 \text{sign}(u) + \mu \frac{du}{dy} \quad (4)$$

where τ_0 denotes the yield stress dependent on the external magnetic field and μ – the fluid viscosity.

Equation (3) implies a linear shear stress distribution across the channel with zero value at the centre as it is shown in Fig. 8a. Due to the yield stress in the fluid, this leads to the development of a plug where the shear stress does not exceed this value. Outside the plug, the fluid behaves in a viscous manner. The predicted flow profile across the channel will depend on the distribution of the yield stress across the channel. The simplest distribution, the constant one, shown schematically

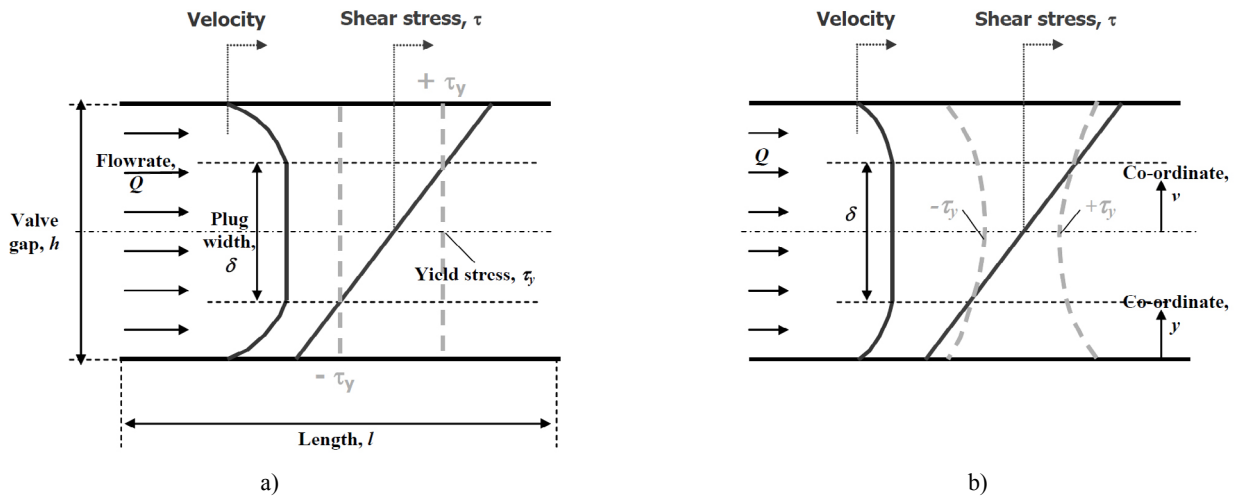


Fig. 8. Schematic diagrams of MR fluid flow between parallel flat plates: a) constant yield stress distribution across the gap, b) quadratic yield distribution across the gap.

in Fig. 8), results from the assumption of the uniform magnetic field. The steady Bingham plastic flow between parallel flat plates when the yield stress remains constant across the gap can be described by the Buckingham equation [7].

As it was shown above in Fig. 7 the magnetic flux density distribution is not uniform, therefore the yield stress distribution across the gap is non-uniform, either. A good approximation of the yield stress distribution can be given by a quadratic function (Fig. 8b) which can be correlated with the distribution of the magnetic flux plotted in Fig. 7. In this case the modified Buckingham equation presented in [7] can be adopted.

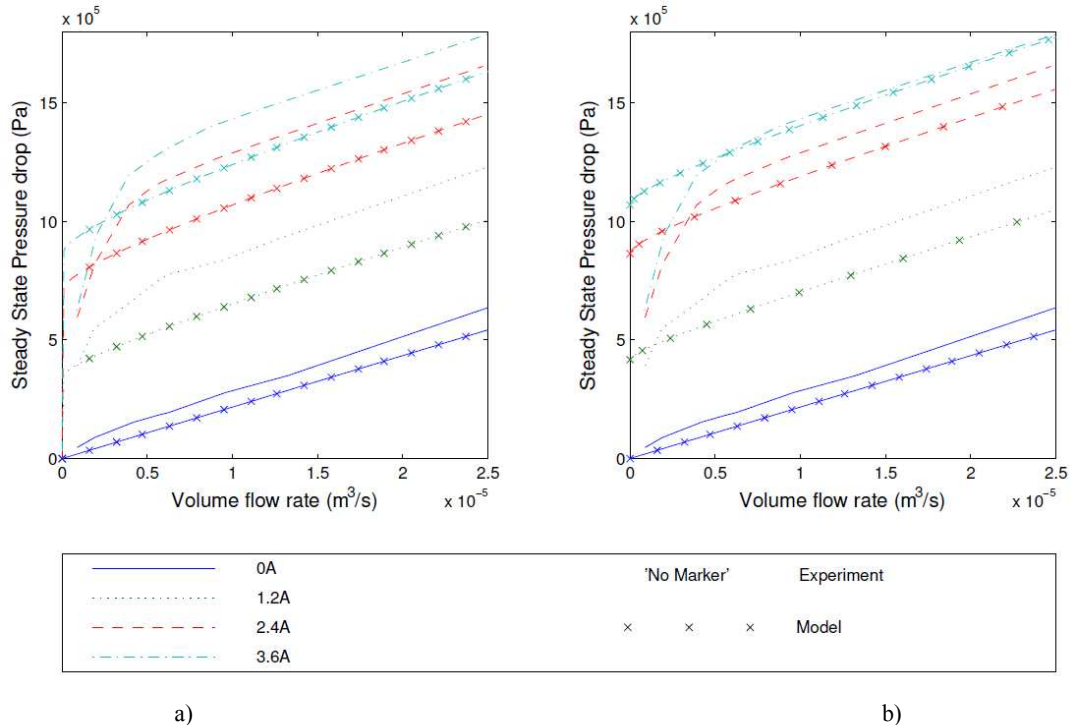


Fig. 9. Comparison of the experimental quasi-steady damping function with (a) the Buckingham equation and (b) the modified Buckingham model.

Detailed solution procedures of the conventional and modified Buckingham equations are given in [8]. The theoretical solutions are compared with experimental results in Fig. 9. It can be observed that the modified Buckingham model allows us to obtain more accurate solutions than the conventional model based on the assumption of the constant yield stress distribution.

V. DISCRETE ELEMENT MODEL OF MAGNETORHEOLOGICAL FLUIDS

Rheological properties of a MR fluid depend on the induced microstructure of the imbedded ferrous particles. When subject to an external field these particles magnetize and align themselves in chains parallel to the applied magnetic field. The microstructure of these chains is a function of several parameters including particle size, applied magnetic field strength, and viscosity and velocity of the surrounding fluid. In order to study the behaviour of MR fluids at the microscopic level a micromechanical model has been developed within the framework of the discrete element method (DEM) which allows us to consider microstructure of suspension of ferrous particles at different working conditions and take into account effects of the intensity of the applied magnetic field, the particle size and particle volume fraction, the magnetic property of the particle, and the viscosity of the carrier fluid, on the mechanical properties of MR fluids. Analysis of the behaviour of the representative volume element will allow later to determine macroscopic properties: the shear yield stress and viscosity of the MR fluid.

In the DEM a particulate material is represented by a collection of spherical particles interacting by means of short-range forces such as contact ones and long-range interactions such as magnetic ones [11]. The motion of the i -th particle in a MR fluid is described by the Newton's second law of motion

$$m_i \ddot{\mathbf{u}}_i = \mathbf{F}_i \quad (5)$$

where m_i is the particle mass, \mathbf{u}_i – the particle displacement in the fixed coordinate system, and \mathbf{F}_i – the resultant force acting on the particle, being the sum of magnetic interactions with other particles \mathbf{F}_i^m , repelling forces \mathbf{F}_i^c due to contact with other particles or with the walls of the container and the resistance of the fluid \mathbf{F}_i^f :

$$\mathbf{F}_i = \mathbf{F}_i^m + \mathbf{F}_i^c + \mathbf{F}_i^f \quad (6)$$

Magnetic forces

Magnetized particles in the magnetic field are treated as point dipoles with magnetic moments \mathbf{m}_i given by:

$$\mathbf{m}_i = V_i \mathbf{M} \quad (7)$$

where V_i is the particle volume and \mathbf{M} is the intensity of magnetisation of the particle. Magnetisation depends on the magnetic field inside the particle \mathbf{H}_i and the magnetic susceptibility of the particle material χ . For a linearly susceptible material, the induced magnetisation is given by:

$$\mathbf{M} = \chi \mathbf{H}_i \quad (8)$$

The magnetisation curve $M = M(H)$ is usually nonlinear and it can be approximated assuming different functions, for instance that employed in [12]:

$$M(H) = |\mathbf{M}| = M_s \tanh \frac{\chi H_i}{M_s} \quad (9)$$

where M_s is the saturation magnetization of the particles.

The force \mathbf{F} on the point dipole \mathbf{m} in the magnetic field is given by:

$$\mathbf{F} = \nabla(\mathbf{m} \cdot \mathbf{B}) \quad (10)$$

where \mathbf{B} is the magnetic flux density, $\mathbf{B} = \mu \mathbf{H}$, μ being the permeability of the material. The permeability of the carrier fluid can be assumed as equal to that of free space μ_0 . The total magnetic force, \mathbf{F}_i^m , exerted on the particles of the assembly of N magnetized particles is a sum of the force caused by the externally applied magnetic field and magnetic interactions \mathbf{F}_{ij}^m with other particles-dipoles

$$\mathbf{F}_i^m = \mu_0 \nabla(\mathbf{m}_i \cdot \mathbf{H}^{\text{ext}}) + \sum_{j, j \neq i}^N \mathbf{F}_{ij}^m \quad (11)$$

If the externally applied magnetic field is uniform, its gradient is zero, and the first term in (11) vanishes. Then, the magnetic force on the particle i is a resultant of interaction forces with other particles. The interaction force between two point dipoles, \mathbf{m}_i and \mathbf{m}_j is given by the following equation [13], [14]:

$$\mathbf{F}_{ij}^m = \frac{3\mu_0}{4\pi} \left[\frac{(\mathbf{m}_i \cdot \mathbf{r}_{ij})\mathbf{m}_j + (\mathbf{m}_j \cdot \mathbf{r}_{ij})\mathbf{m}_i + (\mathbf{m}_i \cdot \mathbf{m}_j)\mathbf{r}_{ij}}{r_{ij}^5} - 5 \frac{(\mathbf{m}_i \cdot \mathbf{r}_{ij})(\mathbf{m}_j \cdot \mathbf{r}_{ij})\mathbf{r}_{ij}}{r_{ij}^7} \right] \quad (12)$$

In a simplified approach, the so-called fixed-dipole model, the interparticle force is calculated from (12) assuming that the dipole moments are induced by the external field only [15], [13]. A more exact model, the mutual dipole model, takes into account the contribution of particle dipoles to the magnetic field in other particles [15], [12]. In this approach, determination of the dipole moments requires a solution of the system of linear algebraic equations, which makes this model computationally more expensive.

Hydrodynamic forces

Since particles in the MR fluids are very small and particle motion is relatively slow, the Stokes drag model can be assumed for the hydrodynamic interactions between the the carrier fluid on the magnetic particles [12]:

$$\mathbf{F}_i^f = 6\pi R_i \mu (\mathbf{v}_f - \mathbf{v}_i) \quad (13)$$

where \mathbf{v}_i is the velocity of the particle i , R_i – the particle radius, \mathbf{v}_f – the velocity of the carrier liquid at the particle's position and μ – its viscosity.

Evaluation of contact forces

Contact force exerted on the particle i , \mathbf{F}_i^c is a resultant of contact interactions with other particles and walls, \mathbf{F}_{ij}^c :

$$\mathbf{F}_i^c = \sum_{j, j \neq i}^{N_i^c} \mathbf{F}_{ij}^c \quad (14)$$

where N_i^c is a number of objects (particles and walls) being in contact with the particle i .

The contact forces \mathbf{F}_{ij}^c are obtained using a constitutive model formulated for the contact. In the present formulation, frictional contact is neglected, thus the contact force has only a normal component

$$\mathbf{F}_{ij}^c = F^c \mathbf{n}_i, \quad (15)$$

where \mathbf{n}_i is the unit vector normal to the particle surface at the contact point and directed outwards from the particle i . In further considerations to simplify the notation the indices i and ij will be omitted.

The normal contact force F^c is decomposed to the elastic part F^e and to the damping contact force F^d

$$F^c = F^e + F^d. \quad (16)$$

The elastic part of the normal contact force F^e is proportional to the normal stiffness k_n and the penetration of the two particle surfaces g

$$F^e = k_n g. \quad (17)$$

The penetration is calculated as

$$g = d_{ij} - R_i - R_j, \quad (18)$$

where d_{ij} is the distance of the particle centres, and R_i, R_j their radii. In the formulation used in the present study no cohesion is allowed, so no tensile normal contact forces are allowed

$$F^e \leq 0. \quad (19)$$

If $g < 0$, the formula (17) is valid, otherwise $F^e = 0$.

The contact damping force is assumed to be of viscous type

$$F^d = c_n v_{rn} \quad (20)$$

proportional to the normal relative velocity v_{rn} of the centres of the two particles in contact

$$v_{rn} = (\mathbf{v}_j - \mathbf{v}_i) \cdot \mathbf{n}_i. \quad (21)$$

The value of damping c_n can be taken as a fraction ξ of the critical damping C_{cr} for the system of two rigid bodies with masses m_i and m_j , connected with a spring of the stiffness k_n

$$c_n = \xi C_{cr} \quad (22)$$

where the critical damping can be calculated as:

$$C_{cr} = 2\sqrt{\frac{m_i m_j k_n}{m_i + m_j}}. \quad (23)$$

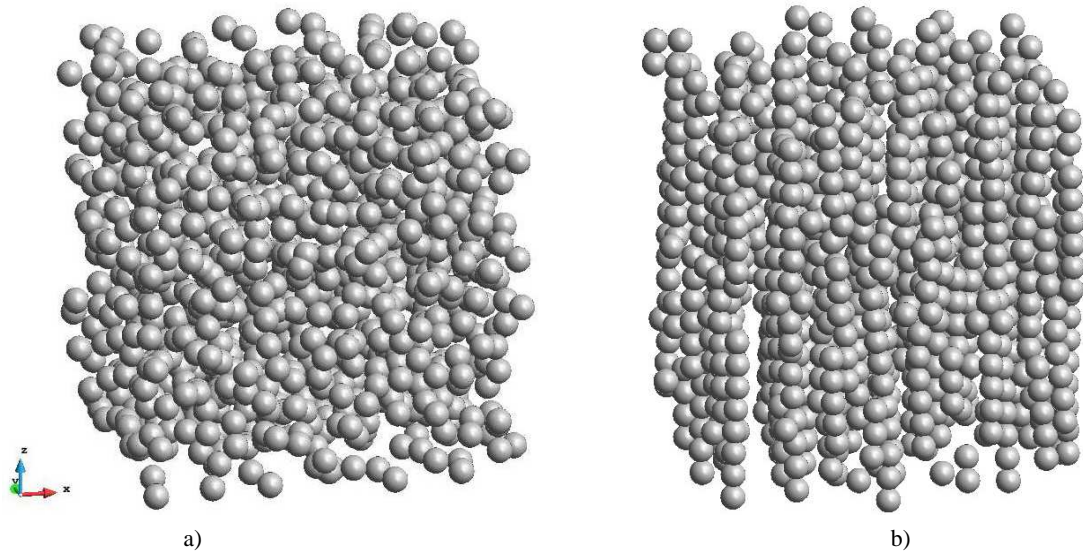


Fig. 10. Discrete element model of a magnetorheological fluid: a) initial random configuration, b) particle chains in the magnetic field

Numerical test

Forming of the particle chains in a MR fluid after application of the magnetic field has been simulated. The purpose of this test was qualitative verification of the performance of the discrete element model developed.

1000 particles of equal size with radii $2.5 \mu\text{m}$ have been generated randomly in a cubic container $80 \times 80 \times 80 \mu\text{m}$. The particle assembly has had porosity of 86.5%. Initial configuration of the particles in the absence of the magnetic field is shown in Figure 10a. The following data have been assumed for the analysis: the magnetic susceptibility of the particle material, $\chi = 5.25$, the saturation magnetisation of the particles $M_s = 2.1/\mu_0 \text{ A/m}$, with $\mu_0 = 4\pi \cdot 10^{-7} \text{ Tm/A}$ being the permeability of free space, particle mass density $\rho = 7800 \text{ kg/m}^3$, and fluid viscosity $\eta = 0.25 \text{ Pa}\cdot\text{s}$. Immobile steady state fluid has been assumed. The magnetic field $H_{ext} = 2 \cdot 10^5 \text{ A/m}$ has been applied in the negative z direction. An interval of 8 ms has been analysed using 500 000 steps. A quasi-static equilibrium with particle chains aligned with the magnetic field lines, has been achieved (Figure 10b). The results confirm a good qualitative performance of the model. Further quantitative tests are planned.

REFERENCES

- [1] T. Butz and O. von Stryk. Modelling and Simulation of Electro- and Magnetorheological Fluid Dampers. *ZAMM Z. Angew. Math. Mech.*, 82:3–20, 2002.
- [2] M.R. Jolly, J.W. Bender, and J.D. Carlson. Properties and applications of commercial magnetorheological fluids. *Journal of Intelligent Material Systems and Structures*, 10:5–13, 1999.
- [3] X. Zhu, X. Jing, and L. Cheng. Magnetorheological fluid dampers: A review on structure design and analysis. *Journal of Intelligent Material Systems and Structures*, 23:839–873, 2012.
- [4] G. Mikułowski and J. Holnicki-Szulc. Adaptive landing gear concept – feedback control validation. *Smart Materials and Structures*, 16:2146–2158, 2007.
- [5] G. Mikułowski and Ł. Jankowski. Adaptive landing gear: optimum control strategy and potential for improvement. *Shock and Vibration*, 16:175–194, 2009.
- [6] J. Holnicki-Szulc, C. Graczykowski, G. Mikułowski, A. Mróz, and P. Pawłowski. Smart technologies for adaptive impact absorption. *Solid State Phenomena*, 154:187–194, 2009.
- [7] H.P. Gavin. Design method for high-force electrorheological dampers. *Smart Materials and Structures*, 7:664–673, 1998.
- [8] G. Mikułowski and D.C. Batterbee. Flux density variation in magnetorheological fluid devices. In C. Mota Soares et al W. Ostachowicz, J. Holnicki-Szulc, editor, *III ECCOMAS Thematic Conference on Smart Structures and Materials*, Gdańsk, Poland, 2002.
- [9] FEMM. Foster-Miller, Inc., Waltham, MA, USA, 2005.
- [10] G. Astarita and G. Marrucci. *Principles of non-Newtonian fluid mechanics*. McGraw-Hill, 1974.
- [11] J. Rojek, C. Labra, O. Su, and E. Oñate. Comparative study of different discrete element models and evaluation of equivalent micromechanical parameters. *International Journal of Solids and Structures*, 49:1497–1517, 2012.
- [12] H.G. Lager, C. Bierwisch, and M. Moseler. MRF in plate-plate magnetorheometer: Numerical insight into the particle-wall interface. *Journal of Physics: Conference Series*, 412:012020, 2013.
- [13] H. Li and X. Peng. Numerical Analysis and Accelerated Approaches in the Simulation of Particle Dynamics in MR Fluids. *Journal of Information & Computational Science*, 7:1669–1678, 2010.
- [14] K. Han, Y.T. Feng, and D.R.J. Owen. Three-dimensional modelling and simulation of magnetorheological fluids. *Int. J. Num. Meth. Eng.*, 84:1273–1302, 2010.
- [15] E.E. Keaveny and M.R. Maxey. Modeling the magnetic interactions between paramagnetic beads in magnetorheological fluids. *Journal of Computational Physics*, 227:9554–9571, 2008.